ChemComm

COMMUNICATION

View Article Online
View Journal | View Issue

Cite this: *Chem. Commun.*, 2024, **60**, 404

Received 6th October 2023,
Accepted 28th November 2023

DOI: 10.1039/d3cc04920e

rsc.li/chemcomm

Reductive cyclodimerization of chalcones: exploring the "self-adaptability" of galvanostatic electrosynthesis†

Mauro Garbini,[a] Andrea Brunetti,[ab] Riccardo Pedrazzani,[ab] Magda Monari,[ab] Massimo Marcaccio,[ab] Giulio Bertuzzi*[ab] and Marco Bandini*[ab]

The "self-adaptability" of galvanostatic electrolysis was shown to assist a multistage unprecedented chemo- and diastereoselective electrochemically promoted cyclodimerization of chalcones. The process, all involving the reductive events, delivered densely functionalized cyclopentanes featuring five contiguous stereocenters (25 examples, yields of up to 95%, *dr* values up to >20 : 1). Dedicated and combined experimental as well as electrochemical investigation revealed the key role of a dynamic kinetic resolution of the aldol intermediate for the reaction mechanism.

In recent years, the development of effective and sustainable synthetic strategies in organic chemistry has been shown to be tremendously advanced by the diversification of enabling technologies.[1] In particular, the highest potential is reached when the application of different techniques dictates reaction outcomes such as chemoselectivity, product distribution and stereoselectivity. This goal extends the shades of the synthetic palette, allowing a multifaceted chemical space, where the outcome can be easily diversified even when drawing from the same pool of starting materials.

The use of synthetic organic electrochemistry (electroChem) not only replaces stoichiometric oxidizing/reducing chemical agents with electrons as traceless equivalents, but also delivers novel reaction pathways and complementary selectivity.[2] In this scenario, the peculiar features of galvanostatic electrolysis offer a reaction manifold of unparalleled power and simplicity.[3] Self-adapting the reaction potential to the one that is needed for the less demanding process to occur allows for the precise control of cascade processes, even where the subsequent reactive events are energetically more demanding than the previous ones (Fig. 1). This approach has yielded significant landmarks in organic synthesis with applications in non-trivial C–C and C–X bond formations.[4] Moreover, by exercising easy and precise control over the quantity and energy of the electrons participating in a redox process, electroChem is an unparalleled protocol for obtaining insights into reaction pathways, in particular by enabling ready access to the isolation of intermediates in a controlled manner. In contrast, traditional stoichiometric or other redox technologies commonly lack the same "live" adaptability and operational tunability during the chemical event.[5] On the other hand, the use of harsh chemical reagents, capable of covering all potential ranges of the redox-active functional groups, could be detrimental to the overall process selectivity.

In continuation with our recent interests in selective radical processes and electrochemical reaction development,[6] we tackled the exploitation of galvanostatic electrolysis for

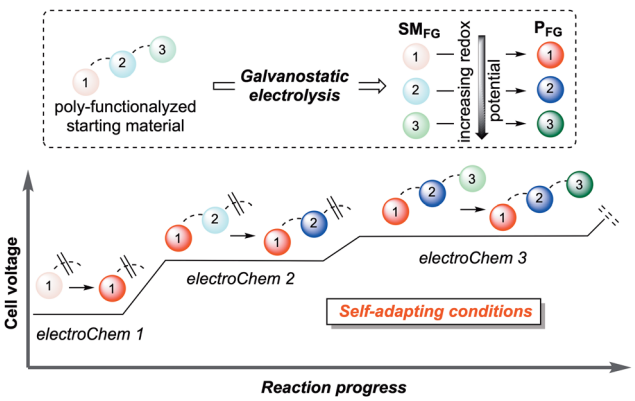

Fig. 1 Pictorial representation of the concept of "self-adaptability" of galvanostatic electroChem utilized in organic synthesis.

[a] *Dipartimento di Chimica "Giacomo Ciamician", Alma Mater Studiorum – Università di Bologna, Via P. Gobetti 85, 40129, Bologna, Italy. E-mail: giulio.bertuzzi2@unibo.it, marco.bandini@unibo.it*
[b] *Center for Chemical Catalysis – C[3], Dipartimento di Chimica "Giacomo Ciamician", Alma Mater Studiorum – Università di Bologna, Via P. Gobetti 85, 40129, Bologna, Italy*

† Electronic supplementary information (ESI) available. CCDC 2290358 and 2290359. For ESI and crystallographic data in CIF or other electronic format see DOI: https://doi.org/10.1039/d3cc04920e

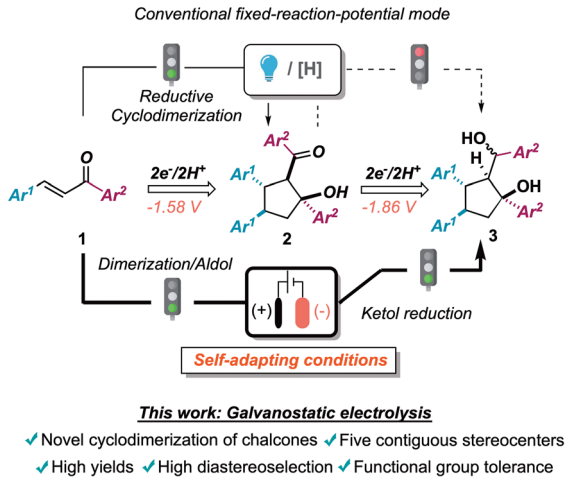

Scheme 1 Electroreductive cyclodimerization of chalcones. The state of the art and the present proposal. [H]: stoichiometric chemical reductive agent.

achieving rapid access to chemical diversity and efficient monitoring of reaction pathways, by investigating the reductive cyclodimerization of chalcones **1**.[7] This machinery was used as a platform to improve and expand reductive synthetic methodologies, featuring chemo-, regio-, and diastereoselectivity issues in the preparation of densely functionalized cyclopentanes (Scheme 1).[8]

In detail, the 1,3-keto alcohol moiety of cyclodimerization products **2** could undergo further reduction to 1,3-diols **3** (*vide infra*). This process, creating a further *exo*cyclic stereocenter, was posited to be more energetically demanding than the first monoelectronic reduction of the extended enone system (*vide infra* for an electrochemical characterization of both starting materials as well as intermediates). Not surprisingly, stoichiometric metal-promoted or photocatalytically assisted reductive conditions led exclusively to aldols **2** (Scheme 1 upper panel). In contrast, self-adaptive galvanostatic electrochemical conditions could yield an elegant way to achieve densely functionalized 1,3-diols **3** featuring five contiguous stereogenic centers (Scheme 1 lower panel).[9]

Despite the intrinsic synthetic challenges posed by this transformation, namely chemoselectivity (**3a** *vs.* **2a**/**2a′** formation) as well as diastereoselectivity (formation of five consecutive stereogenic centers), we were pleased to find that the use of a silver (Ag) cathode and graphite (C) anode, in the presence of triethanolamine (TEOA, 2 equiv.)[7j,10] as a sacrificial reductant (constant current electrolysis, I = 4 mA, 4 F $mol_{\mathbf{1a}}^{-1}$), resulted in the fully chemo- and diastereoselective formation of **3a** in 84% isolated yield (Table 1, entry 1). Importantly, the supporting electrolyte ($TEABF_4$: tetraethylammonium tetrafluoroborate) could be used in a substoichiometric amount (20 mol%, 0.01 M) without consistent issues concerning the medium resistivity. In addition, the reaction could be implemented to the mmol scale with minimal loss of efficiency (yield = 79%).

An extensive survey of reaction parameters (see ESI†) revealed that variations from optimal conditions resulted in a

Table 1 Optimization of reaction conditions[a]

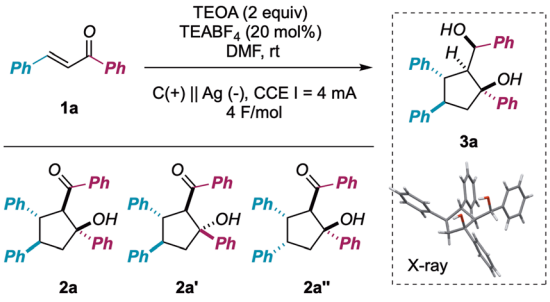

Entry	Deviation from optimal	Y **3a**[b] [%]	**2a**/**2a′**/**2a″**[c]
1	None	84 (79[d])	Traces
2	C_{graph} as cathode	22	—/12/—
3	Ni as cathode	75	Traces
4	$LiBF_4$ as electrolyte	47	Traces
5	$TEABF_4$ (100 mol%)	82	Traces
6	HE as reductant	—	18/17/—
7	Zn as anode, no TEOA	—	33/—/—
8	CCE I = 2 mA	74	—/5/—
9	CCE I = 6 mA	69	Traces
10	DMSO as solvent	69	Traces
11	CH_3CN as solvent	58	Traces

[a] All reactions were carried out in dry solvents and under nitrogen conditions. [b] Isolated yields after flash chromatography. In all cases, **2a** was isolated in >20 : 1 dr as determined from ^{1}H-NMR analysis of the crude reaction products. [c] Yields determined *via* ^{1}H-NMR analysis with mesitylene as an internal standard. [d] Isolated yield for a 1.0 mmol-scale reaction (see ESI for additional details). CCE: constant current electrolysis; HE: Hantzsch ester.

significant drop in reaction performance or no formation of desired product at all. In particular, the importance of using a non-Lewis-acid electrolyte and a metal cathode was underscored for entries 2, 3 and 4, with graphite giving a mixture of **2a″** and **3a** in poor yield and Ni behaving similarly to the optimal Ag. Analogously, using different stoichiometric reductants (entry 6) or a sacrificial anode (entry 7) prevented the formation of the desired product, yielding mixtures of aldols **2** and partial reduction of **1a**. On the other hand, the outcome of the process was found to be less reliant on the intensity of the current (entries 8 and 9) or the reaction solvent (entries 10 and 11), always furnishing diol **3a**, although with diminished efficiency.

Once optimal reaction conditions were established, the generality of the electroreductive cyclodimerization was assessed on a range of densely functionalized chalcones **1b–x** (Scheme 2). Apart from a few cases, the target products **3** were isolated as single diastereoisomers in good to excellent yields (up to 95%). In particular, high tolerance toward electronic perturbations of the electron-deficient double bond, *via* decoration of the adjacent aryl group, was observed. Electron-donating substituents, including alkyl (**1b–c**), phenyl (**1d**), methoxy (**1h**,**m**) and mercaptomethyl (**1i**) groups placed at the *para* or *meta* positions of the arenes, provided a smooth formation of the products **3** (43–80% yields). Electron-poor arenes bearing CF_3 (**1e**), ester (**1f**) cyano (**1g**) and halogen substituents (F, Cl, Br **1k–n**) performed equally well (59–84% yields). Finally, an

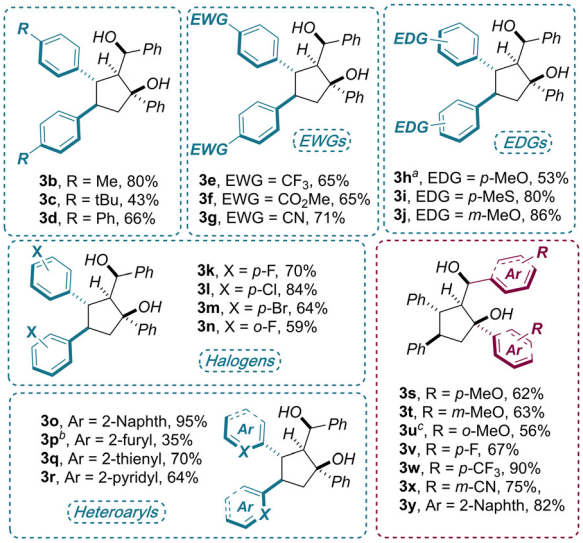

Scheme 2 Reaction scope: reaction conditions as in Table 1, entry 1. Isolated yields were determined after flash chromatography. All compounds were isolated essentially as a single diastereoisomer ($dr > 20:1$) unless otherwise specified: [a] $dr = 8.0:1$. [b] $dr = 11:1$. [c] $dr = 4.4:1$.

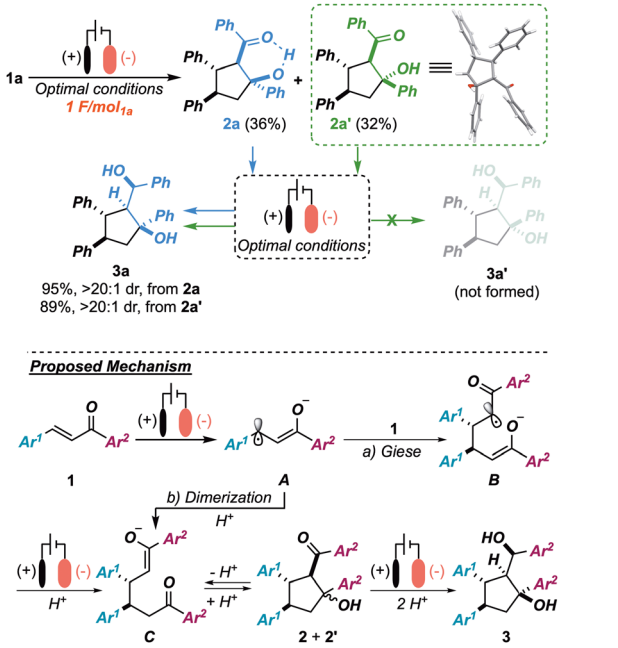

Scheme 3 Upper panel: control experiments proving the electrochemical dynamic resolution. Lower panel: overall picture of the tentative operating mechanism.

extended π-system (**1o**), as well as electron-rich heteroarenes (furan and thiophene, **1p**, **q**) and electron-poor pyridine (**1r**), were also well tolerated in the disclosed protocol (35–95% yields).

Variations of the aromatic ketone moiety of **1** were also investigated by means of testing substrates **1s–y**. Here, when subjecting electron-rich (**1s–u**) and electron-poor (**1v–x**) chalcones to the optimized conditions, good to excellent yields (62–90%) were obtained regardless of the functional group position. In fact, *ortho*, *meta* and *para* substitutions did not affected significantly the outcome of the process, with only a slight drop in diastereoselectivity (4.4 : 1) with product **3u**.

In order to shed light on the mechanism of the whole process—and, in particular, on the key unprecedented late-stage reduction to **3**—we monitored the progress of the reaction over time. To our surprise, by simply interrupting the reaction after providing 1 F $mol_{\mathbf{1a}}^{-1}$, an equimolar mixture of diastereoisomers $\mathbf{2a}^{7h-k}$ and **2a′** was observed (68% combined yield). Isomer **2a′** was unambiguously identified as an epimer of **2a** *via* a single-crystal X-ray diffraction analysis (Scheme 3 upper-right), thus showing a lack of diastereoselectivity in the aldol cyclization stage. This evidence resulted in sharp contrast with the highly diastereoselective outcome observed at the end of the cascade (**3a**, $dr > 20:1$). Interestingly, by re-subjecting either isomer **2a** or **2a′** to the optimized conditions independently, **3a** was isolated in a diastereoselective manner ($dr > 20:1$) in both cases and no traces of the putative epimer **3a′** (theoretically **2a′** → **3a′**) were observed. Thus, both **2a** and **2a′** were deemed to be productive intermediates in the formation of **3a** and, while **2a** was reduced directly to the final target, **2a′** is believed to undergo a retro-aldol ring opening event, responsible for an equilibration between **2a** and **2a′**.[11] Following these experimental results, the tentative mechanism depicted in the lower panel of Scheme 3 is porposed. Accordingly, after a monoelectronic reduction of chalcone **1a** (radical anion **A**), a tail-to-tail Giese addition to a second molecule of **1a** (intermediate **B**) is postulated, giving, after a second cathodic event and protonation, the 1,6-diketone monoenolate **C** (pathway a). Alternatively, **C** can be directly produced (after protonation) from a radical-radical coupling of **A**, given the high concentration of this species at the cathode surface (pathway b). Hereafter, **C** is thought to undergo a non-diastereoselective intramolecular aldol cyclization, followed by a dynamic kinetic resolution of the intermediates resulting from an irreversible ketone reduction. This hypothesis could be rationalized in terms of higher reactivity of isomer **2a**, relative to **2a′**, toward the reductive step, probably due to the formation of an activating intramolecular hydrogen bond being possible only in the former isomer. Moreover, note that in the present machinery, TEOA would act both as a sacrificial reductant as well as protic source, whenever needed.[7j,10]

In this framework, a preliminary electrochemical investigation deploying cyclic voltammetry was carried out on chalcone **1a** and intermediate **2a** (Fig. S3, ESI†). The analysis of the cyclic voltammetric curve of **1a** showed a completely chemically irreversible process ($E_{pc} = -1.52$ V *vs.* SCE) followed by a broad and partially reversible voltammetric wave, made of two closely spaced processes, with a height of about half of the first irreversible reduction. To account for the proton exchange stages involved in the mechanism (formation of **C**, followed by an aldol cyclization), an experiment with a controlled concentration of H_2O was carried out.

Here, the second peak was made completely reversible and occurred at $E_{\frac{1}{2}} = -1.86$ V. The cyclic voltammetric curve of **2a**

was also recorded under the same conditions, and showed a reversible reduction at the same potential ($E_{\frac{1}{2}} = -1.86$ V) as that of the second voltammetric wave of chalcone **1a**. Interestingly, the voltammetric analysis supported the first steps of the mechanism depicted in Scheme 3. In particular, the reduction of **1a** (formation of intermediate **A**) was concluded to be followed by a dimerization of the radical anion **A** and proton exchange (Scheme 3, pathway b).[12,13] Finally, the exocyclic ketone moiety of the newly formed product(s) **2** can undergo a reduction process. All these steps agree both with the redox potentials recorded and the half height of the second voltammetric peak with respect to the first one.

In conclusion, we have demonstrated that the "self-adaptability" of galvanostatic electrolysis is a compelling tool for the realization of cascade processes with a high level of chemo- and stereocontrol. Under these conditions, a new route for the reductive cyclodimerization of chalcones was developed, leading to cyclopentane scaffolds, in high yields (up to 95%) and diastereocontrol ($dr > 20:1$) over five contiguous stereocenters. The tunability of reaction conditions allowed us to shed light on the whole operating electrochemically mediated mechanism, revealing a dynamic kinetic resolution of the intermediate aldol products by means of the final irreversible reduction.

We thank the University of Bologna and Consorzio CINMPIS for their support. GB is also grateful to the PRIN-2022 project (20227Z3BL8) for financial support.

Conflicts of interest

There are no conflicts to declare.

Notes and references

1 (*a*) C. O. Kappe, J. Mack and C. Bolm, *J. Org. Chem.*, 2021, **86**, 14242 (all dedicated issue); (*b*) S. G. Newmann, *Enabling Tools and Techniques for Organic Synthesis: A Practical Guide for Experimentation Automation, and Computation*, Wiley, 2023; (*c*) L. Grimaud, S. Lakhdar and M. R. Vitale, *Curr. Opin. Elctrochem.*, 2023, **40**, 101307.

2 (*a*) M. Yan, Y. Kawamata and P. S. Baran, *Chem. Rev.*, 2017, **117**, 13230; (*b*) A. Wiebe, T. Gieshoff, S. Möhle, E. Rodrigo, M. Zirbes and S. R. Waldvogel, *Angew. Chem., Int. Ed.*, 2018, **57**, 5594; (*c*) C. Kingston, M. D. Palkowitz, Y. Takahira, J. C. Vantourout, B. Y. Peters, Y. Kawamata and P. S. Baran, *Acc. Chem. Res.*, 2020, **53**, 72; (*d*) R. D. A. Little, *J. Org. Chem.*, 2020, **85**, 13375; (*e*) Y. Yuan and A. Lei, *Nat. Commun.*, 2020, **11**, 802; (*f*) L. F. Novaes, J. Liu, Y. Sgen, L. Lu, J. M. Meinhardt and S. Lin, *Chem. Soc. Rev.*, 2021, **50**, 7941; (*g*) M. C. Leech and K. Lam, *Nat. Rev. Chem.*, 2022, **6**, 275; (*h*) L. Zheng, J. Wang, D. Wang, H. Yi and A. Lei, *Angew. Chem., Int. Ed.*, 2023, e20230962; (*i*) R. Franche and Curr Opin, *Electrochem.*, 2023, **36**, 101111; (*j*) P. K. Baroliya, M. Dhaker, S. Panja, S. A. Al-Thabaiti, S. M. Albukhari, Q. A. Alsulami, A. Dutta and D. Maiti, *ChemSusChem*, 2023, **16**, e202202201; (*k*) Y. Li, S. Dana and L. Ackermann, *Curr. Opin. Electrochem.*, 2023, **40**, 101312; (*l*) C. E. Hatch and W. C. Chain, *ChemElectroChem*, 2023, **10**, e202300140.

3 For a general review, see: (*a*) M. Rafiee, M. N. Mayer, B. T. Punchihewa and M. R. Mumau, *J. Org. Chem.*, 2021, **86**, 15866; See also: (*b*) K. D. Moeller, *Tetrahedron*, 2000, **56**, 9527; (*c*) B. H. Nguyen, R. J. Perkins, J. A. Smith and K. D. Moeller, *Beilstein J. Org. Chem.*, 2015, **11**, 280; (*d*) Q.-L. Yang, Y.-Q. Li, C. Ma, P. Fang, X.-J. Zhang and T.-S. Mei, *J. Am. Chem. Soc.*, 2017, **139**, 3293.

4 (*a*) Z.-W. Hou, Z.-Y. Mao, J. Song and H.-C. Xu, *ACS Catal.*, 2017, **7**, 5810; (*b*) S. Blank, Z. Nguyen, D. G. Boucher and S. D. Minteer, *Curr. Opin. Electrochem.*, 2022, **35**, 101049; (*c*) P. L. Norcott, *Chem. Commun.*, 2022, **58**, 2944; (*d*) Z. Lin, U. Dhawa, X. Hou, M. Surke, B. Yuan, S.-W. Li, Y.-C. Liou, M. J. Johansson, L.-C. Xu, C.-H. Chao, X. Hong and L. Ackermann, *Nat. Commun.*, 2023, **14**, 4224; (*e*) C. Zhang, D. Chen, J.-P. Wan and Y. Liu, *Synthesis*, 2023, 2911.

5 For selected reviews comparing photo- and electrochemical protocols, see: (*a*) R. H. Verschueren and W. M. De Borggraeve, *Molecules*, 2019, **24**, 2122; (*b*) J. Liu, L. Lu, D. Wood and S. Lin, *ACS Cent. Sci.*, 2020, **6**, 1317; (*c*) N. E. S. Tai, D. Lehnherr and T. Rovis, *Chem. Rev.*, 2022, **122**, 2487.

6 (*a*) Y. Liu, S. Battaglioli, L. Lombardi, A. Menichetti, G. Valenti, M. Montalti and M. Bandini, *Org. Lett.*, 2021, **23**, 4441; (*b*) S. Battaglioli, G. Bertuzzi, R. Pedrazzani, J. Benetti, G. Valenti, M. Montalti, M. Monari and M. Bandini, *Adv. Synth. Catal.*, 2022, **364**, 720; (*c*) L. Lombardi, A. Kovtun, S. Mantovani, G. Bertuzzi, L. Favaretto, C. Bettini, V. Palermo, M. Melucci and M. Bandini, *Chem. – Eur. J.*, 2022, **28**, e202200333G; (*d*) L. Lombardi, A. Cerveri, R. Giovanelli, M. Castiñeira Reis, C. Silva López, G. Bertuzzi and M. Bandini, *Angew. Chem., Int. Ed.*, 2022, **61**, e202211732; (*e*) G. Bertuzzi, G. Ombrosi and M. Bandini, *Org. Lett.*, 2022, **24**, 4354; (*f*) A. Brunetti, G. Bertuzzi and M. Bandini, *Synthesis*, 2023, **55**, 3047–3055; (*g*) L. Rapisarda, A. Fermi, P. Ceroni, R. Giovanelli, G. Bertuzzi and M. Bandini, *Chem. Commun.*, 2023, **59**, 2664.

7 For stoichiometric low-valent metal induced protocols see: (*a*) K. Takaki, F. Beppu, S. Tanaka, Y. Tsubaki, T. Jintoku and Y. Fujiwara, *J. Chem. Soc., Chem. Commun.*, 1990, **6**, 516; (*b*) K. Takaki, K. Nagase, F. Beppu and Y. Fujiwara, *Chem. Lett.*, 1991, 1665; (*c*) L.-H. Zhou, D.-Q. Shi, Y. Gao, W.-B. Shen, G.-Y. Dai and W.-X. Chen, *Tetrahedron Lett.*, 1997, **38**, 2729; (*d*) L. Zhou and Y. Zhang, *Synth. Commun.*, 2000, **30**, 597; (*e*) L. Moisan, C. Hardouin, B. Rousseau and E. Doris, *Tetrahedron Lett.*, 2002, **43**, 2013; (*f*) K. K. Kapoor, S. Kumar and B. A. Ganai, *Tetrahedron Lett.*, 2005, **46**, 6253; (*g*) Y.-J. Chen, L.-T. Wu, T.-A. Li, M.-Q. Pu, X.-L. Sun, H. Bao and W.-M. Wan, *Angew. Chem., Int. Ed.*, 2023, **62**, e202304033; for photocatalytic methodologies see: (*h*) G. Zhao, C. Yang, L. Guo, H. Sun, R. Lin and W. Xia, *J. Org. Chem.*, 2012, **77**, 6302; (*i*) G. K. Hodgson and J. C. Scaiano, *ACS Catal.*, 2018, **8**, 2914; (*j*) B. Kurpil, Y. Markushyna and A. Savateev, *ACS Catal.*, 2019, **9**, 1531For seminal electrosynthetic reports, targeting (unselectively) products 2, see: (*k*) F. Fournier, J. Berthelot and J.-J. Basselier, *Tetrahedron*, 1985, **41**, 5667; (*l*) J. H. P. Hutley, C. Z. Smith and M. Motevalli, *J. Chem. Soc., Perkin Trans. 2*, 2000, 1053.

8 On the relevance of related cyclopentane scaffolds see: (*a*) Å. Rosenquist, B. Samuelsson, P.-O. Johansson, M. D. Cummings, O. Lenz, P. Raboisson, K. Simmen, S. Vendeville, H. de Kock, M. Nilsson, A. Horvath, R. Kalmeijer, G. de la Rosa and M. Beumont-Mauviel, *J. Med. Chem.*, 2014, **57**, 1673; (*b*) L. Zhou, Y. Tuo, Y. Hao, X. Guo, W. Tang, Y. Xue, J. Zeng, Y. Zhou, M. Xiang, J. Zuo, G. Yao and Y. Zhang, *Org. Lett.*, 2017, **19**, 3029.

9 L. Wang, X. Zhang, R. Y. Xia, C. Yang, L. Guo and W. Xia, *Synlett*, 2022, 1302.

10 (*a*) Y. Pellegrin and F. Odobel, *C. R. Chim*, 2017, **20**, 283; (*b*) S. Mazzanti, B. Kurpil, B. Pieber, M. Antonietti and A. Savateev, *Nat. Commun.*, 2020, **11**, 1387; (*c*) O. Savateev and Y. Zou, *ChemistryOpen*, 2022, **11**, e202200095.

11 A control experiment carried out on pure **2a′** through exposition to TEOA (2 equiv.) furnished a 1 : 1 **2a** : **2a′** mixture.

12 Pathway a in Scheme 3 is also in accordance with the present voltammetric profile, provided that the reduction of **B** to **C** happens at a less negative potential compared to the reduction of chalcone **1a** to radical anion **A**.

13 (*a*) J.-M. Savéant, *Elements of molecular and biomolecular electrochemistry*, Wiley, 2006; (*b*) C. Bruno, E. Ussano, G. Barucca, D. Vanossi, G. Valenti, E. A. Jackson, A. Goldoni, L. Litti, S. Fermani, L. Pasquali, M. Meneghetti, C. Fontanesi, L. T. Scott, F. Paolucci and M. Marcaccio, *Chem. Sci.*, 2021, **12**, 8048.